unibz
Fakultät für Wirtschaftswissenschaften
Facoltà di Economia
Faculty of Economics and Management

BEMPS –
Bozen Economics & Management
Paper Series

NO 100/2023

Global money supply and energy and non-energy commodity prices: A MS-TV-VAR approach

Stefano Grassi, Francesco Ravazzolo, Joaquin Vespignani, Giorgio Vocalelli

Global money supply and energy and non-energy commodity prices: A MS-TV-VAR approach*

Stefano Grassi

Department of Economics and Finance, University of Rome Tor Vergata, Italy

Francesco Ravazzolo

Department of Data Science and Analytics, BI Norwegian Business School, Norway

Faculty of Economics, Free University of Bozen-Bolzano, Italy

Joaquin Vespignani

Tasmanian School of Business and Economics, University of Tasmania, Australia

Centre for Applied Macroeocnomics Analysis, ANU, Australia

Giorgio Vocalelli

Department of Economics, University of Verona, Italy

July 2023

Abstract

This paper shows that the impact of the global money supply is disproportionally high for energy than for non-energy commodities prices. An increase in the global money supply for energy commodity prices results mainly in demand-pull inflation. However, for non-energy commodity prices, an increase in global money supply leads to demand-pull and cost-push inflation, as energy is a key input for non-energy commodities. To quantify this effect, we use a Markov switching model with time-varying transition probabilities. This model considers periods of slow, moderate, and fast global money supply growth. We find that the response to global money supply shocks is almost double for energy than for non-energy commodity prices. We also find heterogeneous responses for energy and non-energy commodities under different regimes.

Keywords: Global money supply; Energy and non-energy prices; Markov-Switching VAR.
JEL codes: C54; E31; F01; Q43.

*We thank Hilde Christiane Bjørnland, Daniel Ventosa-Santaularia, and Francesco Violante for comments and suggestions on this paper. We also thank seminar participants at University of Rome Tor Vergata and University of Verona and participants of the ICEEE 2023 conference in Cagliari. All errors are our own.

1 Introduction

Understanding and quantifying the impact of the global money supply on commodity prices is vital for monetary and fiscal policies. Commodity prices are important causes of macroeconomic fluctuations, such as inflation. Central banks are increasingly coordinating global monetary policies in response to global financial and economic developments (see, for example, Kose et al., 2003, Taylor, 2013, Rey, 2015, and Miranda-Agrippino and Rey, 2020). The Great Recession (2008) and the Covid-19 pandemic (2020) showed greater coordination among central banks, leading to an extraordinary increase in global money supply. In empirical macroeconomic studies, a common result is that increases in money supply lead to commodity prices overshooting (see, for example, the pioneering work of Frankel and Hardouvelis, 1983 and Frankel, 1984). In this paper, we look at this money-driven overshooting of commodity prices through the lenses of energy and non-energy commodity prices. We argue that an increase in the global money supply for energy commodity prices results only in demand-pull inflation. In contrast, for non-energy commodity prices, an increase in global money supply leads to demand-pull inflation and cost-push inflation, as energy prices are a key input in all non-energy commodities (such as agriculture, raw material, fertilizers, precious metals, metals, and minerals). Consequently, the impact of the global money supply is expected to be larger for energy commodity prices than for non-energy commodity prices.

Since the seminal work of Hamilton (1983), extensive research has been conducted on the relationship between economic activity, monetary policy, and commodity prices. However, most studies focus on the impact of commodity prices on *country-specific* monetary policy and economic activity, see Herrera et al. (2019) and references therein. Bernanke et al. (1997) find that the recession effects associated with rising oil prices in the US, is mainly due to a tighter monetary policy. In recent studies, the importance of oil as a driving force behind macroeconomic fluctuations has been further confirmed by Bjørnland et al. (2018). On the contrary, there is a limited literature that explores the impact of global money supply on commodity prices.

The literature on the relationship between money supply and commodity prices dates back to the pioneering works of Frankel and Hardouvelis (1983) and Frankel (1984), who

propose a theoretical model of *overshooting* in commodity markets. As commodities trade in competitive and efficient financial markets, they react to unanticipated movements of money growth in the short term more than proportionally. Moreover, theoretical arguments suggest that an increase in monetary aggregates leads to a rise in aggregate demand, resulting in higher prices of various assets, including commodities. Barsky and Kilian (2002) propose that monetary policy can impact commodity prices by shaping expectations for higher economic growth and inflation. Figure 1 shows the monthly growth of the global money supply, together with the percentage logarithmic returns of the commodity index at the same frequency, from January 1996 to October 2020. It should be noted that significant changes in the money supply can anticipate changes in commodity prices. As suggested by Frankel and Hardouvelis (1983) and Frankel (1984), commodity prices react more than proportionally to changes in the money supply. The most prominent example was during the global financial crisis, when the money supply suffered a significant contraction followed by a considerable drop in commodity prices. Similar patterns can be observed in the first months of 2010 and 2015, respectively.

Sousa and Zaghini (2007) find that a permanent increase in global price is associated with an increase in global money supply. Similarly, Darius (2010) and Belke et al. (2010) find that global money supply shocks impact commodity prices. Ratti and Vespignani (2013) show that monetary shocks in BRIC countries have a more pronounced effect on commodity prices than monetary shocks in G3 economies. However, these studies are carried out within a linear framework, neglecting the possibility that the response can vary depending on the phases of economic activity. An exception is Beckmann et al. (2014), who study the relationship between money supply and commodity prices, setting a Markov Switching (MS) Error Correction model in which the short-term dynamic is subject to regime shifts. Specifically, Beckmann et al. (2014) find evidence of two regimes that they identify as a regime in which commodity prices respond to disequilibria and a regime in which they do not.

We propose a MS-VAR with time-varying transition probabilities to estimate the impact of the global money supply on energy and non-energy commodity prices. Using our model, we identify three regimes underlying money supply, namely periods of slow, moderate, and

fast money supply growth. This sheds light on the quantitative impact of the global money supply on commodity prices at different stages of the global business cycle and provides information to policy makers and the private sector. Our results suggest that energy commodity prices have the highest response (almost twice) in terms of magnitude compared with non-energy commodity prices. After one year, the impact of one standard deviation increase of an unanticipated global money supply shock is associated with a 20.3%(11.3%) increase in energy (non-energy) prices in the slow-money supply regime. For the moderate money-supply regime, the impact of one standard deviation increase of an unanticipated global money supply shock is associated with a 15.6%(7.4%) increase in energy (non-energy) commodity prices. Finally, in the fast money-supply regime, the impact of one standard deviation increase in an unanticipated global money supply shock is associated with a 14.0%(6.0%) increase in energy (non-energy) commodity prices. Therefore, we present a plausible theoretical explanation of why the impact of unanticipated global money supply shocks is larger for energy than for non-energy commodity prices.

The remainder of this paper is organized as follows: in Section 2, we present the transmission mechanism of unanticipated global money supply shocks on energy and non-energy commodity prices. In Section 3, we introduce the MS-VAR model with time-varying transition probabilities and its relative estimation procedure. Section 4 describes the data. In Section 5, we present evidence from three regimes that drive the money supply variable. In Section 6 we inspect the effect of an unanticipated shock of global money supply on commodity (energy and non-energy together) prices within each regime. In Section 7, the heterogeneous responses of different commodity prices to money supply shock are reported. Finally, in Section 8, the conclusions are drawn.

2 The transmission mechanism of an unanticipated global money supply shocks on energy and non-energy commodity prices

In this section, we present the mechanism that leads the impact of money supply shock on energy commodity prices to be more pronounced than on non-energy commodity prices. As in Frankel (1986), an unanticipated increase in the money supply leads to higher expected

inflation. Since commodity prices are not as sticky as other goods, the higher demand for commodities increases prices. However, we show that the money supply shock has a heterogeneous effect on energy and non-energy commodity prices.

Energy commodities are by far the largest commodity market in the world. For example, the capitalization of the crude oil market reached 1.41 trillion US dollars in 2021. Within the energy market, fossil fuel energy (oil, coal, and gas) accounted for approximately 85% of global energy consumption in 2021, according to Ritchie et al. (2022).

Energy commodities are a key input in all non-energy commodities, such as agriculture, raw materials, fertilizers, precious metals, metals, and minerals.[1] A remarkable example is agriculture commodities, which are sectors that require energy directly in the form of fuel and electricity, as well as indirectly through energy-intensive inputs such as fertilizers and pesticides and transport. Similarly, precious metals, other metals, mineral extraction, and exploration depend highly on energy. As a result, an increase in the global money supply affects energy and non-energy commodity prices differently. For energy commodity prices, an increase in global money supply leads to an increase in demand (demand-pull inflation). For non-energy commodity prices, an increase in global money supply leads to an increase in demand (demand-pull inflation) but also to a shift in supply (or cost-push inflation).

Figure 2 shows the different responses of energy and non-energy commodity prices to a global increase in the money supply. Figure 2(a) shows that when the global money supply increases, the demand for energy commodities shifts from D' to D''. The intersection of Q'' and P'' is the new equilibrium E''. The impact of an increase in global money supply on the non-energy commodity is illustrated in Figure 2(b). This figure shows that for non-energy commodities, an increase in global money supply led to an increase in demand from D' to D'' and prices from P' to P''. However, because energy commodities are an input to production of non-energy commodities, S' shifts to the left to S'' reflecting a higher cost of production due to an increase in the cost of energy inputs. This change in supply (and its respective price increase) reduces demand toward the new equilibrium E'''. Consequently, the final equilibrium for energy commodity prices is higher than for

[1]Note that we use the definitions of the World Bank where energy commodities are oil, coal, and gas, and non-energy commodities include agriculture (beverages, food, grains, and other foods), the raw material (wood and other raw materials), fertilizers, precious metals, and metals and minerals. See: Commodity Markets (worldbank.org) for more details.

non-energy commodities.

3 The methodology

To assess the impact of an increase in global money supply on energy and non-energy commodity prices, we use the MS model, see Hamilton (1989) and Krolzig (1997), among others. MS models, which allow parameters to vary according to regimes, are powerful tools for modeling economic expansions and contractions. The MS literature is vast, and it proceeds in both directions: methodological and empirical. From a methodological perspective, the baseline MS model introduced by Hamilton (1989) has been extended to allow transition probabilities to vary over time, see Kaufmann (2015), Billio et al. (2016), and Bazzi et al. (2017). From an empirical point of view, although MS models have been used to study the impact of an energy price shock on macroeconomic quantities (Kilian, 2008, Hamilton, 2011), the literature overlooks the effect of global money supply on commodity prices. This is, to the best of our knowledge, the first attempt to study the impact of global money supply on energy and non-energy commodity prices within an MS framework with time-varying transition probabilities.

3.1 The model

Let $\{\mathbf{y}_t\}_{t=1}^T$ denote a time series of K-variate economic observations. We assume that the probability distribution of $\{\mathbf{y}_t\}_{t=1}^T$ depends on the realizations of a latent discrete-time Markov chain process. The reduced form of the MS-VAR model reads as follows:

$$\mathbf{y}_t = \mathbf{a}(s_t) + \sum_{p=1}^{P} \mathbf{A}_p \mathbf{y}_{t-p} + \boldsymbol{\varepsilon}_t, \quad \boldsymbol{\varepsilon}_t \sim \mathcal{N}_K\left(\mathbf{0}, \boldsymbol{\Sigma}(s_t)\right), \tag{1}$$

where $\mathbf{a}(s_t)$ is a $K \times 1$ vector of intercepts with $s_t \in \{1, \ldots, M\}$ being the realizations of a latent Markov chain process; $\mathbf{A}_p$ is a $K \times K$ matrix containing the autoregressive coefficients where p is the number of lags; $\mathcal{N}_K(\cdot, \cdot)$ denotes a K-variate Normal distribution; and $\boldsymbol{\Sigma}(s_t)$ is a $K \times K$ variance-covariance matrix. Following Krolzig et al. (2000), Billio et al. (2016), and Baştürk et al. (2014), we allow intercepts and the variance-covariance matrix to vary

across regimes and restrict the autoregressive coefficients to be regime-independent. This assumption is motivated by Clements and Krolzig (1998), who show that the intercept mainly drives forecast errors.

The stochastic properties of the latent Markov chain are described by the $(M \times M)$-matrices of time-varying transition probabilities:

$$\mathbf{P}_t = \begin{bmatrix} p_{t,11} & p_{t,12} & \cdots & p_{t,1M} \\ p_{t,21} & p_{t,22} & \cdots & p_{t,2M} \\ \vdots & \vdots & \ddots & \vdots \\ p_{t,M1} & p_{t,M2} & \cdots & p_{t,MM} \end{bmatrix}, \tag{2}$$

with $p_{t,ij} = \mathbb{P}(s_t = i | s_{t-1} = j, \mathbf{V_t}, \boldsymbol{\theta}^{ij})$, $\forall i, j \in \{1, \ldots, M\}$ where $\mathbf{V}_t$ is a set of N exogenous variables and $\boldsymbol{\theta}^{ij}$ is a vector of parameters. Following Kaufmann (2015) and Billio et al. (2016), we model the time-varying transition probabilities using a Logit specification. Accordingly, a centered parameterisation of the transition probabilities, in which exogenous variables drive the time variation of the transition probabilities, is assumed as follows:

$$p_{t,ij} = \frac{\exp\left((\mathbf{V}_t - \mathbf{c})' \boldsymbol{\theta}_1^{ij} + \theta_0^{ij}\right)}{\sum_{i=1}^{M} \exp\left((\mathbf{V}_t - \mathbf{c})' \boldsymbol{\theta}_1^{ij} + \theta_0^{ij}\right)}, \quad i, j = 1, \ldots, M, \tag{3}$$

where $\boldsymbol{\theta}^{ij} = \left(\theta_0^{ij}, \boldsymbol{\theta}_1^{ij'}\right)'$ and $\mathbf{c}$ is a vector of threshold parameters chosen to be the average of $\mathbf{V}_t$. For identification purposes, we let M be the reference regime. We assume that the vectors containing the parameters which drive the transition to the reference regime are null, i.e., $\boldsymbol{\theta}^{Mj} = \mathbf{0}$, $\forall j = 1, \ldots, M$.[2]

As standard in the MS literature, the model is re-parametrized using a partition of the set of regressors to simplify the estimation procedure's exposition. In particular, $(1, \mathbf{y}_{t-1}', \ldots, \mathbf{y}_{t-p}')$ is divided into $M + 1$ subsets: $\overline{\mathbf{x}}_{0t} = \left(\mathbf{y}_{t-1}', \ldots, \mathbf{y}_{t-P}'\right)'$, a $KP \times 1$ vector of regime-independent coefficients, and $\overline{\mathbf{x}}_{it} = 1, i = 1, \ldots, M$, which are M vectors of one regime-specific regressors. Finally, let $\boldsymbol{\xi}_t = (\xi_{1,t}, \ldots, \xi_{M,t})'$ be the vector of indicator functions which contains information regarding the realization of the latent Markov chain

[2]Please note that for $\boldsymbol{\theta}_1^{ij} = 0$, $\forall i, j = 1, \ldots, M$, the MS-VAR with time-varying transition probabilities reduces to the case with constant probabilities.

process, s_t, namely, $\xi_{i,t} = \mathbb{I}_{s_t=i}$, for $i = 1, \ldots, M$ and $t = 1, \ldots, T$, and rewrite the model in Equation (1) as follows:

$$\mathbf{y}_t = \mathbf{X}_{0t}\boldsymbol{\gamma}_0 + \sum_{i=1}^{M} \xi_{it}\mathbf{X}_{it}\boldsymbol{\gamma}_i + \boldsymbol{\varepsilon}_t, \quad \boldsymbol{\varepsilon}_t \sim \mathcal{N}_M\left(\mathbf{0}, \boldsymbol{\Sigma}\left(\boldsymbol{\xi}_t\right)\right), \tag{4}$$

where: $\mathbf{X}_{0t} = (\mathbf{I}_K \otimes \overline{\mathbf{x}}'_{0t})$ and $\mathbf{X}_{it} = \mathbf{I}_K$ are, respectively, the regime-invariant and regime-specific regressor matrices; $\boldsymbol{\gamma}_0 = \text{vec}\left((\mathbf{A}_1, \ldots, \mathbf{A}_P)'\right)'$ are the regime-invariant autoregressive parameters; $\boldsymbol{\Sigma}\left(\boldsymbol{\xi}_t\right) = \boldsymbol{\Sigma}\left(\boldsymbol{\xi}_t \otimes \mathbf{I}_K\right)$ where $\boldsymbol{\Sigma} = (\boldsymbol{\Sigma}_1, \ldots, \boldsymbol{\Sigma}_M)$ with $\boldsymbol{\Sigma}_i$ being the $K \times K$ regime-specific variance-covariance matrix, and $\boldsymbol{\Sigma}(s_t) = \sum_{i=1}^{M} \boldsymbol{\Sigma}_i \xi_{it}$, see Equation (1); finally $\boldsymbol{\gamma}_i = \mathbf{a}_i$ is a vector $K \times 1$ containing the regime-dependent equation intercepts, and $\mathbf{a}(s_t) = \sum_{i=1}^{M} \mathbf{a}_i \xi_{it}$, see Equation (1).

3.2 Bayesian inference

Given the generous parameterisation of the MS-VAR model introduced in Section 3.1, the estimation strategies are based on Bayesian techniques. The possibility of restricting parameters with different prior beliefs makes Bayesian methods a powerful tool in macroeconomics to overcome overfitting issues that arise from many free parameters and short time series, see Ciccarelli and Rebucci (2003).

We set up a Gibbs sampler algorithm to draw from the conditional posterior distributions, particularly we use the multi-move strategy to filter the latent regimes (Chib, 1996, Krolzig, 1997). The conditional posterior distribution from which parameters are sampled is recovered by combining the complete data likelihood $p(\mathbf{y}, \boldsymbol{\Xi}|\boldsymbol{\phi})$, where $\boldsymbol{\phi} = (\boldsymbol{\gamma}, \boldsymbol{\Sigma}, \boldsymbol{\theta})$, with the prior distribution $p(\boldsymbol{\phi})$ as follows:

$$p(\boldsymbol{\phi}, \boldsymbol{\Xi}|\mathbf{y}) \propto p(\mathbf{y}, \boldsymbol{\Xi}|\boldsymbol{\phi})p(\boldsymbol{\phi}), \tag{5}$$

where: $\mathbf{y} = \text{vec}(\mathbf{y}_1, \ldots, \mathbf{y}_T)$ is the vector $TK \times 1$ that contains the observation; $\boldsymbol{\Xi} = (\boldsymbol{\xi}_1, \ldots, \boldsymbol{\xi}_T)$ is the vector $MT \times 1$ of the indicator variables; $\boldsymbol{\gamma} = \text{vec}(\boldsymbol{\gamma}_1, \ldots, \boldsymbol{\gamma}_M)$ is a vector of the regressor coefficients; and $\boldsymbol{\theta}$ contains the parameters of the time-varying

transition probabilities. Moreover:

$$p\left(\mathbf{y}, \boldsymbol{\Xi}|\boldsymbol{\phi}\right) = (2\pi)^{-\frac{TK}{2}} \prod_{t=1}^{T} \left|\boldsymbol{\Sigma}\left(s_t\right)\right|^{-\frac{1}{2}} \exp\left\{-\frac{1}{2}\mathbf{u}_t'\boldsymbol{\Sigma}\left(s_t\right)^{-1}\mathbf{u}_t\right\} \prod_{i=1}^{M}\prod_{j=1}^{M} p_{ij}^{\xi_{it}\xi_{jt-1}}, \tag{6}$$

and $\mathbf{u}_t = \mathbf{y}_t - \left((1, \boldsymbol{\xi}_t') \otimes \mathbf{I}_K\right)\mathbf{X}_t\boldsymbol{\gamma}$, with:

$$\mathbf{X}_t = \begin{pmatrix} \mathbf{X}_{0t} & \mathbf{X}_{1t} & \dots & \mathbf{0} \\ \vdots & \vdots & \ddots & \vdots \\ \mathbf{X}_{0t} & \mathbf{0} & \dots & \mathbf{X}_{Mt} \end{pmatrix}. \tag{7}$$

The Gibbs sampler is divided into four steps. We first draw from the conditional posterior distribution of the VAR coefficients, $\boldsymbol{\gamma}_0$, independent of the hidden Markov chain. Second, we draw the state-dependent intercepts, $\boldsymbol{\gamma}_i$, together with the variance-covariance matrix, $\boldsymbol{\Sigma}_i$. Then, we draw, from the conditional posterior distribution of the parameters of the transition probabilities, $\boldsymbol{\theta}^{ij}$. Finally, the fourth step draws the vector of latent states, $\boldsymbol{\Xi}$. Defining $\boldsymbol{\gamma}_{(-i)} = (\gamma_1, \dots, \gamma_{i-1}, \gamma_{i+1}, \dots, \gamma_M)$ and $\boldsymbol{\Sigma}_{(-i)} = (\boldsymbol{\Sigma}_1, \dots, \boldsymbol{\Sigma}_{i-1}, \boldsymbol{\Sigma}_{i+1}, \dots, \boldsymbol{\Sigma}_M)$ we can sketch here the estimation algorithm:

1) Draw $\boldsymbol{\gamma}_0$ from $f(\boldsymbol{\gamma}_0|\mathbf{y}, \boldsymbol{\Xi}, \boldsymbol{\gamma}_{(-i)}, \boldsymbol{\Sigma})$;

2) For $i = 1, \dots, M$:

   (a) draw $\boldsymbol{\gamma}_i$ from $f(\boldsymbol{\gamma_i}|\mathbf{y}, \boldsymbol{\Xi}, \boldsymbol{\gamma}_{(-i)}, \boldsymbol{\Sigma})$;

   (b) draw $\boldsymbol{\Sigma}_i^{-1}$ from $f\left(\boldsymbol{\Sigma}_i^{-1}|\mathbf{y}, \boldsymbol{\Xi}, \boldsymbol{\gamma}_i, \boldsymbol{\Sigma}_{(-i)}\right)$;

3) Draw $\boldsymbol{\theta}^{j1}, \dots, \boldsymbol{\theta}^{j(M-1)}$ from $f\left(\boldsymbol{\theta}^{j1}, \dots, \boldsymbol{\theta}^{j(M-1)}|\mathbf{y}, \boldsymbol{\Xi}, \boldsymbol{\gamma}_i\right)$;

4) Draw $\boldsymbol{\Xi}$ from $p\left(\boldsymbol{\Xi}|\mathbf{y}, \boldsymbol{\gamma}, \boldsymbol{\Sigma}, \boldsymbol{\theta}\right)$.

The full posterior distributions in 1) to 3) are given in Appendix B, while the latent states are sampled using the multi-move sampling strategy (Chib, 1996; Krolzig, 1997). When dealing with mixture models in a Bayesian framework, the estimation must explicitly treat the invariance of the likelihood under relabeling of the mixture components to avoid the so-called label switching problem, see Redner and Walker (1984) and Frühwirth-Schnatter (2006). To address the problem of label switching, we constrain the intercept

of the global money supply equation, α_i^{GL}, $\forall i = 1, \ldots, M$, to increase between regimes, namely $\alpha_1^{GL} < \alpha_2^{GL} < \ldots < \alpha_M^{GL}$. Imposing this restriction implies that the conditional mean of global money supply growth is lower in the first regime and increases between regimes when moving to the Mth regime. This assumption is consistent with our objective to distinguish between periods of slow and fast money supply growth.

4 Data

Following Ratti and Vespignani (2015), we construct the global money supply variable using M2 denominated in US dollars of the seven largest economies worldwide (China, EU, India, Japan, Russia, the UK, and the US) as measures of money supply.[3] These data are sampled monthly, the highest frequency available, from January 1996 to October 2020, and Thomson Reuters provides them. Global money supply (GM2) is constructed as the sum of national monetary aggregates as follows:

$$GM2_t = \sum_{i=1}^{N} M2_{i,t}, \quad t = 1, \ldots, T, \tag{8}$$

where $M2_{i,t}$ is the aggregate measure of M2 money for country i at time t.

To assess the effect of an increase in money supply on commodity (energy and non-energy together) prices, we use the Global Price Index of All Commodities from FRED as a tracker of global commodity prices (GCP). Data on short-term interest rates come from the Federal Reserve Bank of Dallas, particularly from the Database of Global Economic Indicators. The global interest rate is calculated as the sum of the US policy rate and the World (excluding the US) short-term interest rate weighted by their respective share of global GDP as follows:

$$GIR_t = (1 - w_t^{US}) IR_t^{World} + w_t^{US} IR_t^{US}, \tag{9}$$

where the weights w_t^{US} are constructed using the ratio between the quarterly data on

[3]The countries taken into account represent more than the 70% share of the world GDP according to the last published World Bank data paper.

GDP^{US} and GDP^{World}. The weights are assumed to be constant within the quarter, and the data are freely available on the International Monetary Fund website.

Global industrial production (GIP) and the global consumer price index (GCPI) drive the time-varying transition probabilities. Similarly to the global interest rate variable, they are constructed using data from the Global Economic Indicators of the Federal Reserve Bank of Dallas by summing up their respective world and US variables weighted by the share of global GDP. The frequency of the data is monthly, and we use the 3-month growth to have stationary and less volatile data. The vector containing the VAR variables in Equation (1) is given by $\mathbf{y}_t' = [\Delta \ln(GM2_t), \Delta \ln(GIR_t), \Delta \ln(GCP_t)]$, while the transition probabilities are driven by $\mathbf{V}_t' = [\Delta \ln(GIP_t,), \Delta \ln(GCPI_t)]$.

Finally, we used data from the World Bank to study the effects of positive innovation in the global money supply on the prices of different sectors of commodity markets. Specifically, we use data on energy, non-energy, precious metals, agriculture, raw materials, and metals and minerals sectors stored in the "Pink Sheet" dataset of the World Bank.

5 Non-linearities in global money supply

In this section, we present the characteristics of the MS dynamics that drive the global money supply. First, we determine the number of regimes that drive the global money supply by comparing the goodness-of-fit of different model specifications. Second, by inspecting the kernel density estimates of the posterior draws of the regime-dependent parameters, we examine the characteristics of the regime that the model detects. Then, we look at the smoothed probabilities produced by the MS-VAR. Finally, we check the contribution of global economic indicators, GIP and GCPI, to the probabilities of switching between regimes.

5.1 Number of regimes

To find evidence of a non-unique underlying regime that drives global growth in money supply, we compare a standard VAR with a MS-VAR using different model specifications. Then, the in-sample goodness-of-fit of each model is evaluated according to the Deviance

Information Criterion (DIC), introduced by Spiegelhalter et al. (2002). The DIC reads as follows:

$$\text{DIC} \doteq 2\left\{\ln \mathcal{L}\left(\bar{\boldsymbol{\phi}}|\mathbf{y}\right) - 2\mathbb{E}_{\boldsymbol{\phi}|\mathbf{y}}\left[\ln \mathcal{L}\left(\boldsymbol{\phi}|\mathbf{y}\right)\right]\right\}, \tag{10}$$

where $\mathbb{E}_{\boldsymbol{\phi}|\mathbf{y}}[\ln \mathcal{L}(\boldsymbol{\phi}|\mathbf{y})]$ is the expected value with respect to the joint posterior density, $\mathcal{L}(\boldsymbol{\phi}|\mathbf{y})$ is the likelihood, and $\bar{\boldsymbol{\phi}} = \mathbb{E}_{\boldsymbol{\phi}|\mathbf{y}}(\boldsymbol{\phi})$. Following Kaufmann and Frühwirth-Schnatter (2002) the likelihood function in Equation (10) can be rewritten as:

$$\mathcal{L}(\boldsymbol{\phi}|\mathbf{y}) = \prod_{t=1}^{T}\left[\sum_{i=1}^{M} p\left(\mathbf{y}_t|\boldsymbol{\phi}, s_t = i, \mathbf{y}^{t-1}\right)\mathbb{P}\left(s_t = i|\boldsymbol{\phi}, \mathbf{y}^{t-1}\right)\right], \tag{11}$$

where $p\left(\mathbf{y}_t|\boldsymbol{\phi}, s_t = i, \mathbf{y}^{t-1}\right)$ is the distribution of $\mathbf{y}_t$ conditioned to a single realization of the hidden Markov chain, and $\mathbb{P}\left(s_t = i|\boldsymbol{\phi}, \mathbf{y}^{t-1}\right)$ is the filtered probability. Like other information criteria, the DIC balances the goodness-of-fit and model complexity. To identify the best number of latent regimes that drive the global money supply, we estimate the VAR and the MS-VAR with up to sixteen lags and three regimes. Table 1 shows the DIC with the corresponding confidence intervals.

The confidence intervals are constructed following Ardia (2009), which proposes to re-sample the posterior estimates using the stationary block bootstrap of Politis and Romano (1994). This methodology estimates the uncertainty of the DIC without re-computing the model several times, reducing the computational burden. The optimal length of the blocks is selected by applying the Politis and White (2004) methodology to each parameter, using the resulting maximum value as the optimal length. The DIC reported in Table 1 supports the evidence of three regimes. In fact, given the same number of lags, the MS(3)-VAR consistently outperforms the other specifications.

Regarding the order of the autoregressive coefficients, the DIC suggests that sixteen lags fit the data better. However, to avoid possible overfitting problems which may arise using the DIC (Ando, 2007) and to find more conclusive evidence on the number of lags, we also employ predictive likelihood (PL), see Frühwirth-Schnatter (2006). While the DIC tests the goodness-of-fit in the sample, the PL tests the out-of-sample performance. Specifically, we evaluate the PL for the MS(3)-VAR, with $p = 1, \ldots, 16$, and the one with the highest PL delivers the best out-of-sample goodness of fit. The PL suggests that the model with twelve

lags has the best score in terms of PL, see Table 2. Therefore, we choose the MS(3)-VAR with twelve lags.

5.2 Empirical identification of the regimes

Looking at the kernel density estimates of posterior draws, we provide evidence of regime identification. Figure 3 reports the kernel density estimates of the posterior draws of the regime-dependent intercepts.

The first moments of the posterior density of the intercepts of the global money supply equation increase across regimes; each regime represents a different state of the monetary cycle. The red shaded area refers to a period of slow money growth; similarly, the blue and green shaded areas refer to moderate and fast liquidity growth regimes, respectively. The support of global money supply intercepts associated with the second and third regimes is positive and statistically different from zero. This result suggests that in both regimes the global money supply tends to increase.

The regime-dependent intercepts of the commodity price equation are distinguishable across regimes, suggesting that the conditional mean of the commodity price growth is significantly different depending on the phases of the monetary cycle. Specifically, the support of the intercept is negative and statistically different from zero in the first regime, which corresponds to a period of slow money growth. This result indicates that when the global money supply decreases, commodity prices also tend to decrease. In the second regime, the commodity prices intercept is centered around zero, while it is positive and statistically different from zero during periods of fast credit growth.

The intercept of the GIR associated with a period of contraction of credit growth is negative. This interest rate behavior is justified by the fact that in the same period, commodity prices drop, and monetary authorities loosen monetary policy to boost economies. The intercepts supports overlap in the second and third regimes, suggesting no clear difference across them.

Figure 4 shows the other state-dependent parameter, that is, the estimates of the variance-covariance matrices. The residual volatility of GM2, GIR, and GCP is reported. As shown in the figure, there are similarities in the volatility behavior between variables,

and the regimes are also identified from a volatility perspective. The first regime, associated with a contraction in money supply growth, is generally the most volatile period. In periods of money supply bursts, usually caused by a financial crisis, volatility increases as economic activity slows down and uncertainty increases. On the contrary, the second and third regimes are much less volatile. The second regime is the least volatile period for GM2 and GIR, while it is the third regime for GCP. That is, during periods of high credit growth, commodity prices increase steadily.

5.3 Regime probabilities

The smoothed probabilities reported in Figure 5 identify the periods associated with each regime. The upper panel of Figure 5 shows the filtered probabilities, the red dashed, blue dotted, and green solid lines refer to the first, second, and third regimes, respectively. As visible, the first part of the sample is characterized by periods of booms and bursts in GM2 growth; on the contrary, since 2003, global money supply growth has experienced a steady increase interrupted by periods of money contraction during financial distress.

The rise in GM2, which began in 2003, is also recognized as the beginning of the global liquidity cycle (Kokeyne et al., 2010) which had accelerated since 2009 when policymakers around the world began to adopt quantitative easing measures in response to the financial crisis.

Looking at the upper panel of Figure 5, it is worth noting that before the Great Recession of 2009, there was a period of increasing money supply that accelerated just before the crisis and then followed a regime of low credit growth. A similar path can be observed in the early 2000s, namely during the dot-com bubble and the Covid-19 pandemic. As shown in Meller and Metiu (2017), Schularick and Taylor (2012), and Gourinchas and Obstfeld (2012), recessions are often preceded by money booms, usually in tandem with the drying up of money in circulation.

Between 2010 and 2020, the monetary aggregate maintained sustained growth. This was when Western economies implemented unconventional monetary policies and increased money circulation.

In the first two quarters of 2020, with lockdowns in response to the Covid-19 pandemic,

the likelihood of being in a regime of slow money growth is higher. Following the recession, policymakers worldwide implemented expansionary monetary measures to support economies, leading to a fast money supply growth regime.

Finally, in the lower panel of Figure 5, the GCP (black dotted line) and the filtered states (red solid line) are shown. The solid red line takes the value 5 (-5) when it is in the third (first) regime and a value equal to zero when it is in the second regime. As is visible, GCP behaves accordingly to GM2 growth regimes. In particular, they rise when money growth accelerates and decrease accordingly. As shown in the figure, GCP fell after the dot-com bubble, the Great Financial Crisis, and the Covid-19 recession.

5.4 Time-varying transition probabilities

An important feature of the MS-VAR is the transition probabilities that change over time. They are parametrized as in Kaufmann (2015), and we assume that global indicators of economic activity drive the transition probability matrix. In other words, the probability of switching between money supply regimes depends on GIP and the GCPI. Table 3 shows the posterior mean of the parameters associated with each variable, together with the 90% credible interval in parentheses.

First, it should be noted that most coefficients are statistically significant, which means that both variables have a non-trivial effect on the probability of switching between regimes. Furthermore, GIP and the GCPI play a similar role in the probability of switching between regimes.

The first row of Table 3 shows the coefficient associated with GIP and GCPI for the probability of remaining in a low-money supply growth regime or moving from the first regime to a regime of moderate global money supply growth. As is visible, an increase in GCPI and in GIP increases the probability of remaining in the first regime. On the contrary, it reduces the likelihood of entering the second regime. Similarly, $\theta_1^{j2}, j = 1, 2$, and $\theta_2^{j2}, j = 1, 2$, suggest that if the GIP and GCPI increase, the probability of switching from the second regime to the first regime increases, reducing the likelihood of remaining in the second. When the global economy is in a period of fast money supply growth increasing the GCPI and GIP leads to a higher probability of returning to the first or second regime.

6 Structural form

To investigate how an unanticipated money supply shock propagates to commodity prices and vice versa, the reduced model of Equation (1) has to be represented in structural form. Let us consider the following equation:

$$\mathbf{y}_t'\mathbf{B}_0(s_t) = \boldsymbol{x}_t'\mathbf{B}_+(s_t) + \boldsymbol{u}_t', \tag{12}$$

where: $\boldsymbol{x}_t = (1, \mathbf{y}_{t-1}, \ldots, \mathbf{y}_{t-P})$. The parameters $\mathbf{A}(s_t) = (\mathbf{a}(s_t), \mathbf{A}_1, \ldots, \mathbf{A}_p)$ are estimated in reduced form, $\mathbf{A}(s_t)' = \mathbf{B}_+(s_t)\mathbf{B}_0(s_t)^{-1}$, $\boldsymbol{\varepsilon}_t = \mathbf{B}_0(s_t)^{-1}\boldsymbol{u}_t$, and $\boldsymbol{\Sigma}(s_t) = (\mathbf{B}_0(s_t)\mathbf{B}_0(s_t)')^{-1}$. Imposing sufficient conditions on $(\mathbf{B}_0(s_t)\mathbf{B}_0(s_t)')$ the structural form is identified. Nevertheless, the reduced form parameters do not uniquely identify structural parameters and shocks across equations. Therefore, it is impossible to distinguish regime shift from one structural equation to another, see Sims and Zha (2006). To identify shocks, we use the Cholesky decomposition as in Sousa and Zaghini (2007) and Sousa and Zaghini (2008). These studies use a similar identification strategy to examine the impact of unanticipated fluctuations in the G5 monetary aggregate on GDP and inflation and the effect of foreign monetary aggregates on the Euro area economy, respectively. Accordingly, we assume that GCP responds simultaneously to a GM2 shock and a GIR shock, while GM2 reacts to GIR and GCP with a one month lag.

Figure 6 shows the cumulated impulse response functions (IRFs) of GCP and GIR to an increase of one standard deviation in an unanticipated GM2 shock in each regime. As shown in the figure, an unexpected increase in GM2 leads to a temporary increase in GCP in each regime. In the first regime, when monetary growth is slow, the GCP reacts more than in the other regimes. In the long run, the shock is absorbed within 14 months if GM2 is in one of the two increasing regimes, while it is absorbed within about 12 months if GM2 is in the first regime.

In contrast, cumulative IRF of GIR to a one-standard-degree increase from an unanticipated GM2 shock are never statistically significant. At a global level, there is no clear evidence of what is the effect of an increase in GM2 on the GIR. Following the reasoning of Ratti and Vespignani (2015), who find similar results, at the worldwide level, there is no

unique central bank that rules interest rates.

Figure 7 shows the cumulative responses of GM2 and GCP to a one standard deviation increase in an unexpected GIR shock. The figure shows that GM2 does not respond to the increase in GIR, while GCP positively reacts to an unexpected increase in GIR in the first regime. On the contrary, when GM2 is in the second or third regime, it does not respond to commodity prices.

Figure 8 reports the cumulated IRFs of GM2 and GIR to an increase of one standard deviation in an unanticipated GCP shock. A one standard deviation increase in GCP leads to an increase in GIR. When the GCP increases, the monetary authority increases the GIR in response to inflation pressure. The response of GM2 to a GCP shock is unclear and is not statistically significant.

7 The heterogenous effect of global money supply on energy and non-energy commodity prices

In this section, we study the heterogeneous effects of an increase in GM2 on energy and non-energy commodity prices. To do so, we use the same model as in Equation (4), but we substitute GCP with energy and non-energy data. We also include in the analysis data on precious metals, agriculture, raw materials, and metals and minerals.

We report in Figure 9 the cumulated IRFs of energy and non-energy commodity prices to a one standard deviation increase of an unanticipated GM2 shock within each regime[4]. The upper panel shows the median responses of energy and non-energy commodity prices to a positive shock in GM2 in the first regime, the middle panel reports the responses in the second regime, and similarly, in the lower panel, the responses in the third regime are showcased.

Consistently with previous results, both energy and non-energy commodity prices positively react to a one standard deviation increase of an unexpected GM2 shock. Figure 9 shows that after a year, the impact of a one standard deviation increase in GM2 is associated with a 20.3% (11.3%) increase in energy (non-energy) commodity prices in the slow

[4]We report in Appendix C the numerical values of cumulated IRFs, together with their respective credible intervals,

money supply regime. For the moderate money supply regime, the impact of one standard deviation increase in GM2 is associated with an increase of 15.6% (7.4%) in the prices of energy (non-energy) commodities. Finally, for the fast money-supply regime, the same shock is associated with a 14.0% (6.0%) increase in energy (non-energy) commodity prices.

By further inspecting commodities in the non-energy sector, we can see that, after one year, a one standard deviation increase in GM2 in the slow money supply regime leads to a rise of 6.1%, 8.7%, 8.7%, and 9.1% for prices of precious metals, agriculture, raw materials, and metals and minerals, respectively. When the same shock occurs in the moderate money supply regime, after one year, the prices of precious metals, agriculture, raw materials, and metals and minerals increase by 6.4%, 6.7%, 5.4%, and 9.1%. Finally, in the fast money supply growth regime, as a consequence of a one standard deviation GM2 shock, prices for precious metals, agriculture, raw materials, and metals and minerals increase by 5.6%, 5.9%, 6.9%, and 7.8%.

When comparing the magnitude of the shocks, it should be noted that the energy commodity prices tend to respond more strongly to a positive rise in GM2 than the non-energy commodity prices in each regime. In particular, the response size is twice as large as the non-energy price. As shown in Section 2, since energy commodities are a key input of non-energy commodities, an increase in money supply has heterogeneous effects on the prices of energy and non-energy commodities. In fact, an increment of money in circulation increases demand for commodities and increases prices. However, the higher costs faced by non-energy producers reduce the supply of such commodities. Consequently, the shift in supply and its respective price increase reduce demand toward a new equilibrium with lower prices.

8 Conclusions

This paper examines the impact of unanticipated global monetary supply shocks on energy and non-energy commodity prices using a Markov Switching VAR with time-varying transition probabilities based on monthly data from January 1996 to October 2020. We evaluate these unexpected shocks in three different regimes to capture different stages of the global monetary cycle, which can be interpreted as periods when the global money

supply is slow, moderate, and fast.

We present a plausible theoretical explanation of why the impact of unanticipated global money supply shocks is greater for energy than for non-energy commodity prices. We argue that increasing the global money supply for energy commodities results only in demand-pull inflation. In contrast, for non-energy commodities, an increase in global money supply leads to demand-pull inflation and cost-push inflation, as energy commodities are a key input of all non-energy commodities.

Our results indicate that the impact of one standard deviation increase in global money supply is associated with a 20.3% (11.3%) increase in energy (non-energy) commodity prices in the slow-money supply regime after 12 months. For the moderate money-supply regime, the impact of one standard deviation increase in global money supply is associated with a 15.6% (7.4%) in the prices of energy (non-energy) commodities. Finally, for the fast money-supply regime, the impact of one standard deviation increase in the global money supply is associated with a 14.0% (6.0%) increase in energy (non-energy) commodity prices. These heterogeneous results across commodities are very informative to central banks, international organizations, and macroeconomic forecasters who seek to understand the relationship between monetary cycles and commodity prices.

References

Ando, T. (2007). Bayesian Predictive Information Criterion for the Evaluation of Hierarchical Bayesian and Empirical Bayes Models. *Biometrika*, 94:443–458.

Ardia, D. (2009). Bayesian Estimation of a Markov-Switching Threshold Asymmetric GARCH Model with Student-t Innovations. *The Econometrics Journal*, 12:105–126.

Barsky, R. B. and Kilian, L. (2002). Oil and the Macroeconomy Since the 1970s. *Journal of Economic Perspectives*, 18:115–134.

Baştürk, N., Çakmakli, C., Ceyhan, S. P., and Van Dijk, H. K. (2014). Posterior-Predictive Evidence on US Inflation using Extended new Keynesian Phillips Curve Models with Non-Filtered Data. *Journal of Applied Econometrics*, 29:1164–1182.

Bazzi, M., Blasques, F., Koopman, S. J., and Lucas, A. (2017). Time-Varying Transition Probabilities for Markov Regime Switching Models. *Journal of Time Series Analysis*, 38:458–478.

Beckmann, J., Belke, A., and Czudaj, R. (2014). Does Global Liquidity Drive Commodity Prices? *Journal of Banking & Finance*, 48:224–234.

Belke, A., Orth, W., and Setzer, R. (2010). Liquidity and the Dynamic Pattern of Asset Price Adjustment: A Global View. *Journal of Banking & Finance*, 34:1933–1945.

Bernanke, B. S., Gertler, M., Watson, M., Sims, C. A., and Friedman, B. M. (1997). Systematic Monetary Policy and the Effects of Oil Price Shocks. *Brookings papers on economic activity*, 1997:91–157.

Billio, M., Casarin, R., Ravazzolo, F., and Van Dijk, H. K. (2016). Interconnections Between Eurozone and US Booms and Busts Using a Bayesian Panel Markov-Switching VAR Model. *Journal of Applied Econometrics*, 31:1352–1370.

Bjørnland, H. C., Larsen, V. H., and Maih, J. (2018). Oil and Macroeconomic (In) Stability. *American Economic Journal: Macroeconomics*, 10(4):128–151.

Chib, S. (1996). Calculating Posterior Distributions and Modal Estimates in Markov Mixture Models. *Journal of Econometrics*, 75:79–97.

Ciccarelli, M. M. and Rebucci, M. A. (2003). Bayesian VARs: A Survey of the Recent Literature with an Application to the European Monetary System. Technical report.

Clements, M. P. and Krolzig, H.-M. (1998). A Comparison of the Forecast Performance of Markov-Switching and Threshold Autoregressive Models of US GNP. *The Econometrics Journal*, 1:47–75.

Darius, M. R. (2010). *Can Global Liquidity Forecast Asset Prices?* International Monetary Fund.

Frankel, J. A. (1984). Commodity Prices and Money: Lessons from International Finance. *American Journal of Agricultural Economics*, 66:560–566.

Frankel, J. A. (1986). Expectations and Commodity Price Dynamics: The Overshooting Model. *American Journal of Agricultural Economics*, 68:344–348.

Frankel, J. A. and Hardouvelis, G. A. (1983). Commodity Prices, Overshooting, Money Surprises, and Fed Credibility. Technical report, National Bureau of Economic Research.

Frühwirth-Schnatter, S. (2006). *Finite Mixture and Markov Switching Models*. Springer Science & Business Media.

Gourinchas, P.-O. and Obstfeld, M. (2012). Stories of the Twentieth Century for the Twenty-First. *American Economic Journal: Macroeconomics*, 4:226–65.

Hamilton, J. D. (1983). Oil and the Macroeconomy Since World War II. *Journal of political economy*, 91:228–248.

Hamilton, J. D. (1989). A New Approach to the Economic Analysis of Nonstationary Time Series and the Business Cycle. *Econometrica: Journal of the econometric society*, pages 357–384.

Hamilton, J. D. (2011). Nonlinearities and the Macroeconomic Effects of Oil Prices. *Macroeconomic Dynamics*, 15:364–378.

Herrera, A. M., Karaki, M. B., and Rangaraju, S. K. (2019). Oil Price Shocks and US Economic Activity. *Energy policy*, 129:89–99.

Kaufmann, S. (2015). K-state Switching Models with Time-Varying Transition Distributions - Does Loan Growth Signal Stronger Effects of Variables on Inflation? *Journal of Econometrics*, 187:82–94.

Kaufmann, S. and Frühwirth-Schnatter, S. (2002). Bayesian Analysis of Switching ARCH Models. *Journal of Time Series Analysis*, 23:425–458.

Kilian, L. (2008). The Economic Effects of Energy Price Shocks. *Journal of economic literature*, 46:871–909.

Kokeyne, A., Nowak, S., Psalida, E., and Sun, T. (2010). Global Liquidity Expansion: Effects on Receiving Economies and Policy Response Options. *IMF Global Financial Stability Report*.

Kose, M. A., Prasad, E. S., and Terrones, M. E. (2003). How Does Globalization Affect the Synchronization of Business Cycles? *American Economic Review*, 93:57–62.

Krolzig, H.-M. (1997). *Markov-switching Vector Autoregressions: Modelling, Statistical Inference, and Application to Business Cycle Analysis*. Lecture Notes in Economics and Mathematical Systems. New York/Berlin/Heidelberg: Springer.

Krolzig, H.-M. et al. (2000). *Predicting Markov-Switching Vector Autoregressive Processes*. Nuffield College Oxford.

Meller, B. and Metiu, N. (2017). The Synchronization of Credit Cycles. *Journal of Banking & Finance*, 82:98–111.

Miranda-Agrippino, S. and Rey, H. (2020). US Monetary Policy and the Global Financial Cycle. *The Review of Economic Studies*, 87:2754–2776.

Politis, D. N. and Romano, J. P. (1994). The Stationary Bootstrap. *Journal of the American Statistical association*, 89:1303–1313.

Politis, D. N. and White, H. (2004). Automatic Block-Length Selection for the Dependent Bootstrap. *Econometric reviews*, 23:53–70.

Ratti, R. A. and Vespignani, J. L. (2013). Why Are Crude Oil Prices High When Global Activity is Weak? *Economics Letters*, 121:133–136.

Ratti, R. A. and Vespignani, J. L. (2015). Commodity Prices and BRIC and G3 Liquidity: A SFAVEC Approach. *Journal of Banking & Finance*, 53:18–33.

Redner, R. A. and Walker, H. F. (1984). Mixture Densities, Maximum Likelihood and the EM Algorithm. *SIAM Review*, 26:195–239.

Rey, H. (2015). Dilemma Not Trilemma: the Global Financial Cycle and Monetary Policy Independence. Technical report, National Bureau of Economic Research.

Ritchie, H., Roser, M., and Rosado, P. (2022). Energy. *Our World in Data*. https://ourworldindata.org/energy.

Schularick, M. and Taylor, A. M. (2012). Credit Booms Gone Bust: Monetary Policy,Leverage Cycles, and Financial Crises, 1870-2008. *American Economic Review*, 102:1029–61.

Sims, C. A. and Zha, T. (2006). Were there Regime Switches in US Monetary Policy? *American Economic Review*, 96:54–81.

Sousa, J. and Zaghini, A. (2008). Monetary Policy Shocks in the Euro Area and Global Liquidity Spillovers. *International Journal of Finance & Economics*, 13:205–218.

Sousa, J. M. and Zaghini, A. (2007). Global Monetary Policy Shocks in the G5: A SVAR Approach. *Journal of International Financial Markets, Institutions and Money*, 17:403–419.

Spiegelhalter, D. J., Best, N. G., Carlin, B. P., and Van Der Linde, A. (2002). Bayesian Measures of Model Complexity and Fit. *Journal of the royal statistical society: Series b (statistical methodology)*, 64:583–639.

Taylor, J. B. (2013). International Monetary Policy Coordination: Past, Present and Future. Technical report.

Lag	VAR			MS(2)-VAR			MS(3)-VAR		
	5%	DIC	95%	5%	DIC	95%	5%	DIC	95%
2	4639.1	4639.5	4639.8	4371.3	4371.8	4372.5	4330.7	4338.3	4342.9
4	4416.7	4462.2	4462.8	4206.5	4207.2	4207.9	4158.3	4166.1	4178.7
8	4348.3	4348.8	4394.4	4097.0	4097.9	4098.8	4067.0	4070.5	4074.0
12	4275.2	4275.8	4276.4	4026.0	4027.1	4028.3	3982.1	3984.7	3987.7
14	4275.2	4275.8	4276.4	3988.7	3990.3	3991.7	3943.6	3945.5	3948.0
16	4275.2	4275.8	4276.4	3964.3	3966.3	3967.7	3924.3	3927.4	3929.3

Table 1: The Table reports the estimated DIC computed for the Vector Autoregressive Model (VAR), the Markov Switching VAR with two states (MS(2)-VAR), and the Markov Switching VAR with three states (MS(3)-VAR). The table also reports the 5% and the 95% confidence interval constructed using the block-bootstrap of Politis and Romano (1994). The DIC suggests twelve lags for the VAR for all models.

Model	2	4	8	12	14	16
MS(3)-VAR	-2288.6	-2331.0	-2384.0	-2098.5	-2146.2	-2243.4

Table 2: The Table reports the estimated predictive likelihood (PL) computed for the Markov Switching VAR with three states (MS(3)-VAR). The PL suggests twelve lags as the best specification.

Time-varying transition probabilities					
	$\Delta Log(GIP_t)$			$\Delta Log(GCPI_t)$	
	j=1	*j=2*		*j=1*	*j=2*
θ_1^{j1}	0.411	-0.305	θ_2^{j1}	0.383	-0.303
	(0.115, 0.706)	(-0.577, -0.034)		(0.094, 0.686)	(-0.609, -0.002)
θ_1^{j2}	0.407	-0.300	θ_2^{j2}	0.408	-0.298
	(0.107, 0.693)	(-0.585, 0.016)		(0.112, 0.720)	(-0.587, -0.003)
θ_1^{j3}	0.412	0.407	θ_2^{j3}	0.395	0.390
	(0.107, 0.699)	(0.136, 0.694)		(0.111, 0.680)	(0.106, 0.659)

Table 3: Posterior mean and 90% credible interval (in parenthesis) for the coefficients of the variables global industrial production ($\Delta Log(GIP_t)$) and global consumer price index ($\Delta Log(GCPI_t)$) which enter in the dynamic of the transition probabilities.

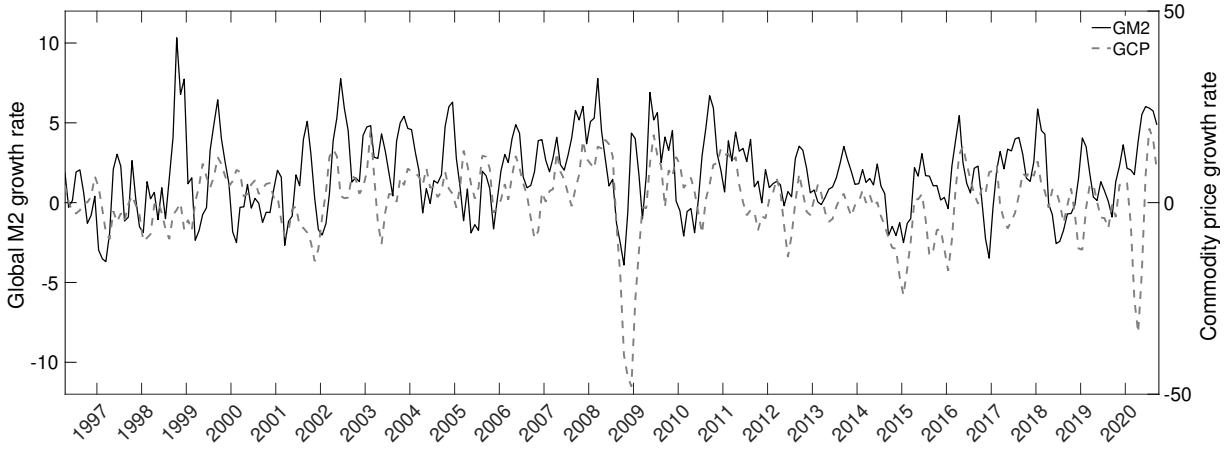

Figure 1: The figure plots the monthly growth rate of global M2 (GM2) with the scale on the left part (black line) and the global commodity index (GCP) with the scale on the right part (grey dashed line), from January 1996 to October 2020.

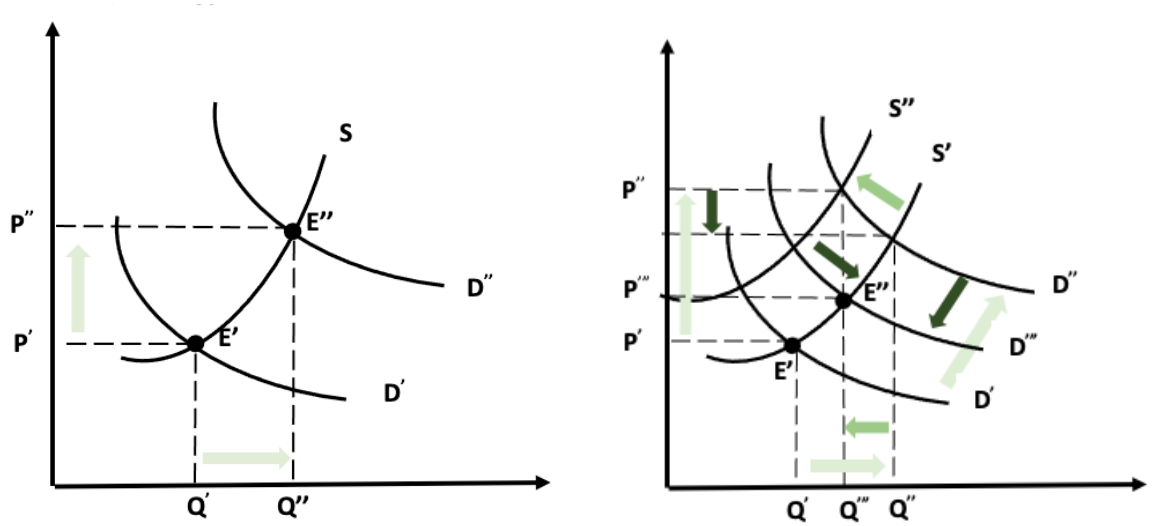

(a) Energy

(b) Non-energy

Figure 2: The X-axis and Y-axis represent the measures of the quantity (Q) produced and prices (P), respectively. Curve S represents the supply, and curve D represents the demand. Panel (a): It shows that energy demand and prices increase in response to an increase in the global money supply. Panel (b): It shows that non-energy demand and prices increase in response to an increase in the global money supply. However, because energy commodities are input into producing non-energy commodities, the supply shifts to the left. Furthermore, this shift in supply reduces demand towards the new equilibrium E'''.

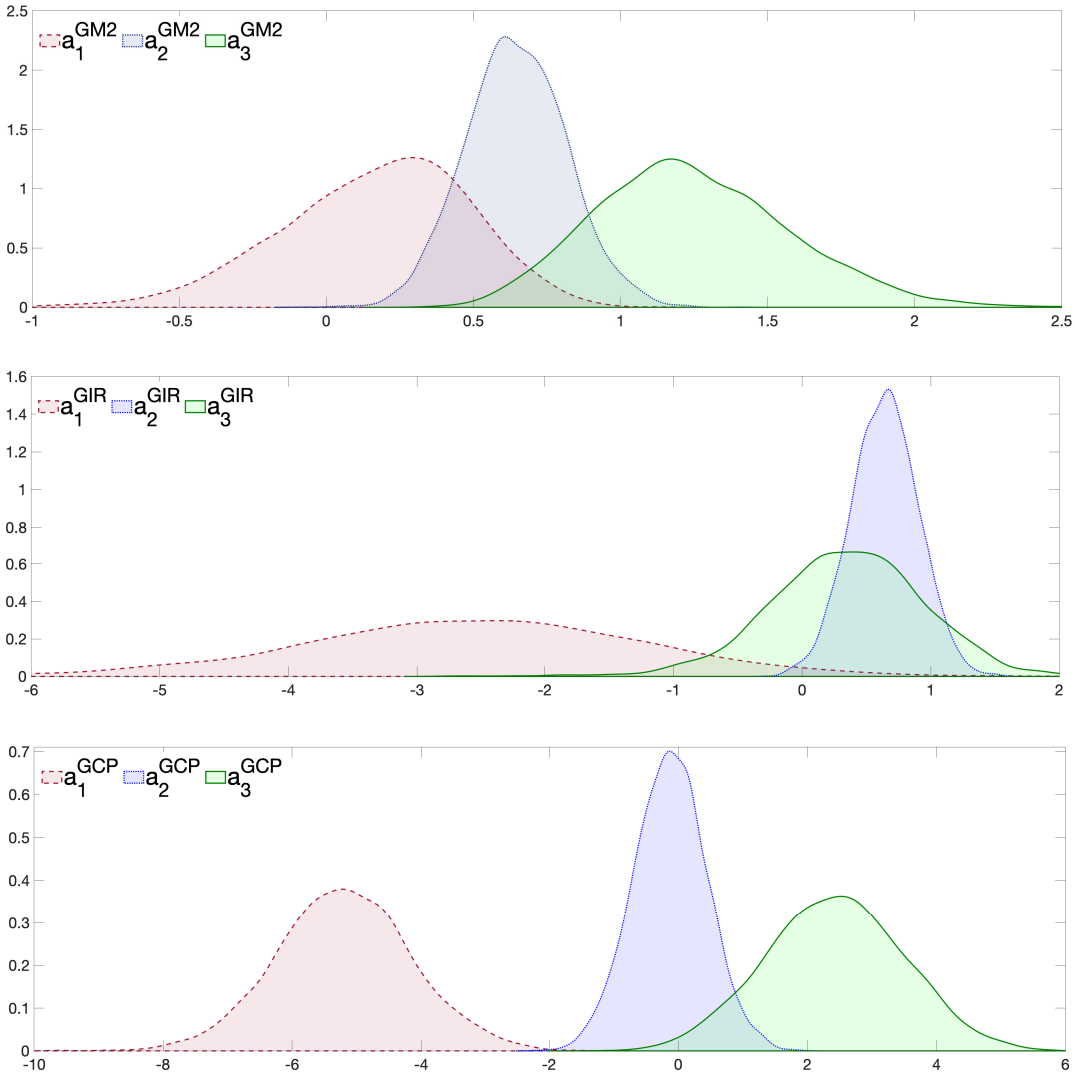

Figure 3: Upper panel: a_1^{GM2}, a_2^{GM2}, and a_3^{GM2} are, respectively, kernel density estimates of the posterior draws of the regime-dependent intercept of the global money supply equation in the first (red shaded area with dashed line), second (blue shaded area with dotted line), and third (green shaded area with continuous line) regimes. Middle panel: a_1^{GIR}, a_2^{GIR}, and a_3^{GIR} are respectively kernel density estimates of the posterior draws of the regime-dependent intercept of the global interest rate equation in the first (red shaded area with dashed line), second (blue shaded area with dotted line), and third (green shaded area with continuous line) regimes. Lower panel: a_1^{GCP}, a_2^{GCP}, and a_3^{GCP} are, respectively, kernel density estimates of the posterior draws of the regime-dependent intercept of the commodity price equation in the first (red shaded area with dashed line), second (blue shaded area with dotted line), and third (green shaded area with continuous line) regimes.

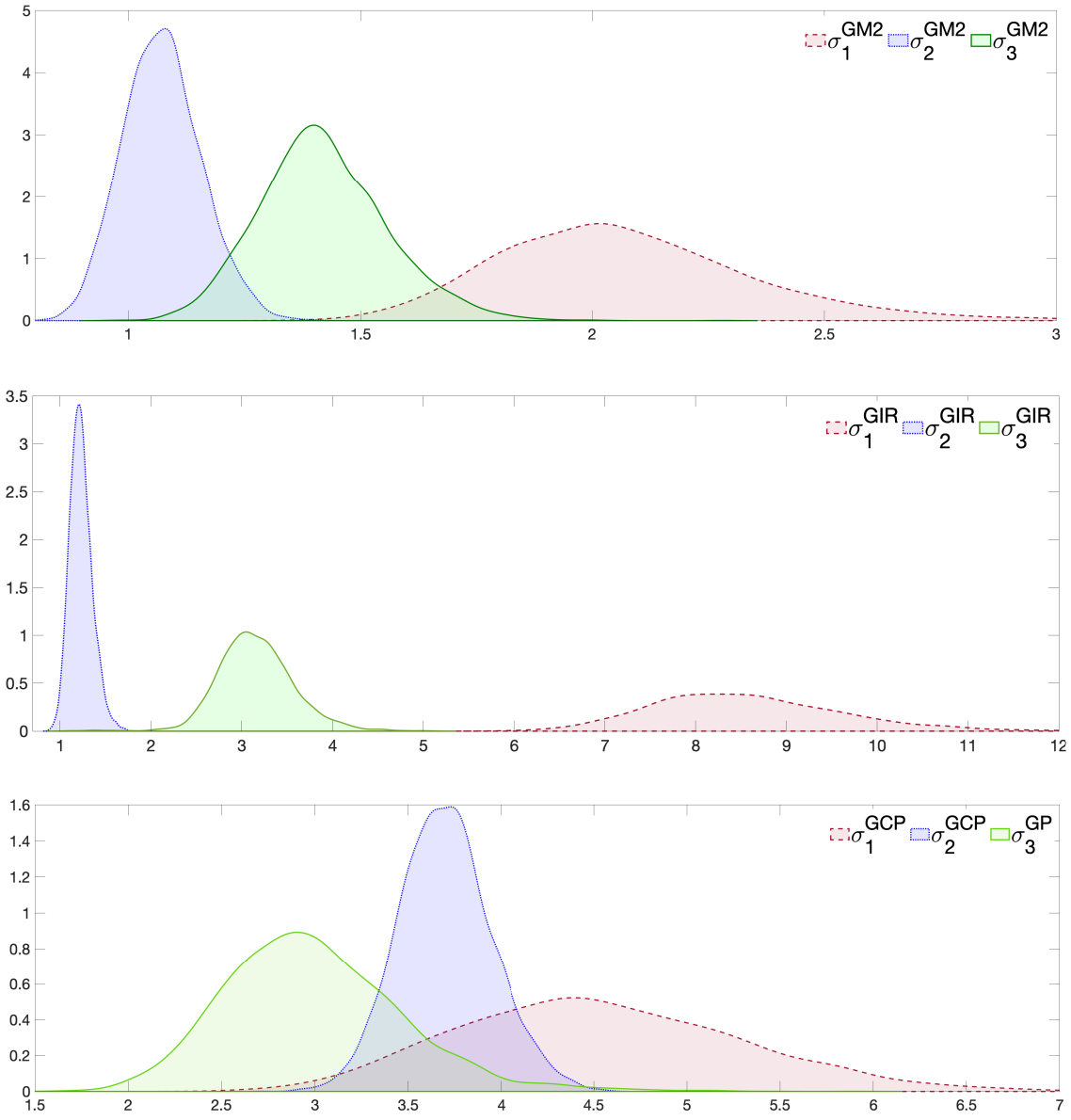

Figure 4: Upper panel: σ_1^{GM2}, σ_2^{GM2}, and σ_3^{GM2} are respectively kernel density estimates of the posterior draws of the regime-dependent standard deviation of global money supply in the first (red shaded area with dashed line), second (blue shaded area with dotted line), and third (green shaded area with continuous line) regimes. Middle panel: σ_1^{GIR}, σ_2^{GIR}, and σ_3^{GIR} are, respectively, kernel density estimates of the posterior draws of the regime-dependent standard deviation of global interest rate in the first (red shaded area with dashed line), second (blue shaded area with dotted line), and third (green shaded area with continuous line) regimes. Lower panel: σ_1^{GCP}, σ_2^{GCP}, and σ_3^{GCP} are, respectively kernel density estimates of the posterior draws of the regime-dependent standard deviation of commodity price in the first (red shaded area with dashed line), second (blue shaded area with dotted line), and third (green shaded area with continuous line) regimes.

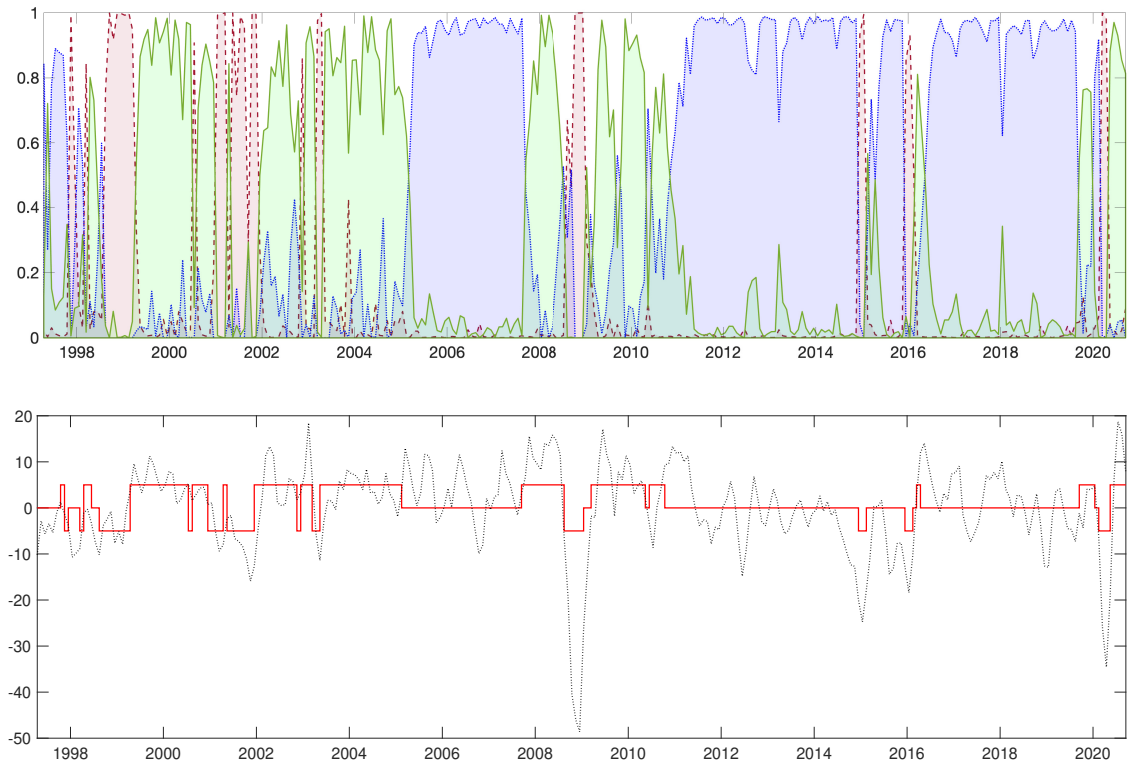

Figure 5: Upper panel: The red shaded area with dashed line refers to the filtered probability of regime 1, the blue shaded area with dotted line is the filtered probability of regime 2, and the green shaded area with continuous line is the filtered probability of regime 3. Lower panel: It shows the growth of commodity prices (black dotted line) and the filtered state (red line). When the red line is 0 indicates evidence of the second regime, when it is equal to -5 indicates evidence of the first regime, and when it is 5, it indicates evidence of the third regime.

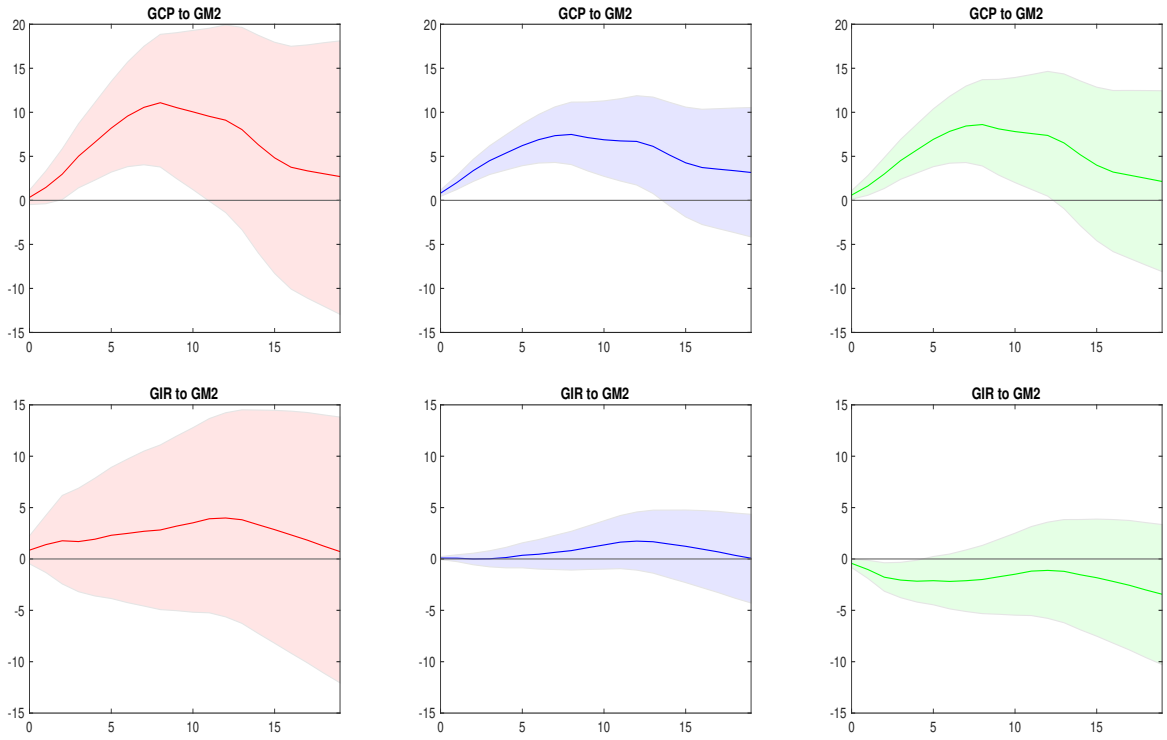

Figure 6: The first and second rows represent the impulse response functions (IRFs) of commodity prices (GCP) and global interest rates (GIR) to the global money supply (GM2) shock, respectively. Each column reports the IRFs in a specific regime. Particularly, on the left are the IRFs in the first regime, on the right are the IRFs in the third regime, and in the middle are the IRFs in the second regime. The solid lines are the median responses, whereas the shaded areas correspond to 68% credible intervals.

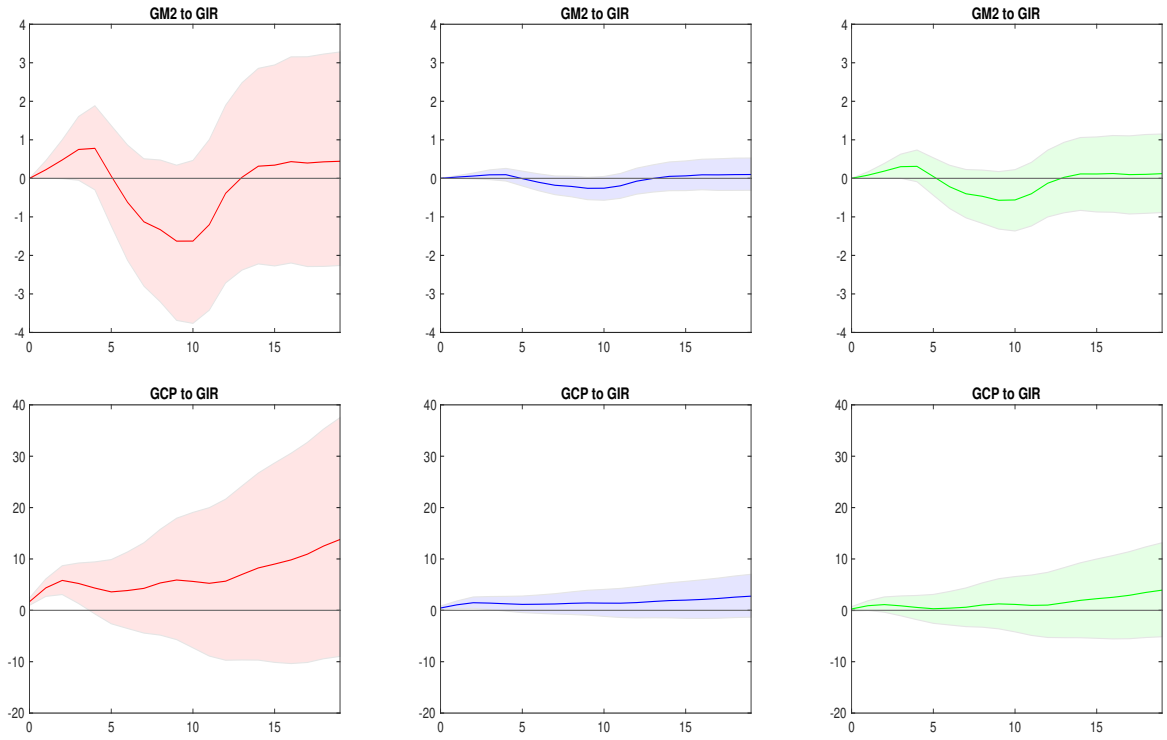

Figure 7: The first and second rows represent the impulse response functions (IRFs) of the global money supply (GM2) and commodity prices (GCP) to a global interest rate (GIR) shock, respectively. Each column reports the IRFs in a specific regime. In particular, on the left are the IRFs in the first regime, on the right are the IRFs in the third regime, and on the middle are the IRFs in the second regime. The solid lines are the median responses, whereas the shaded areas correspond to 68% credible intervals.

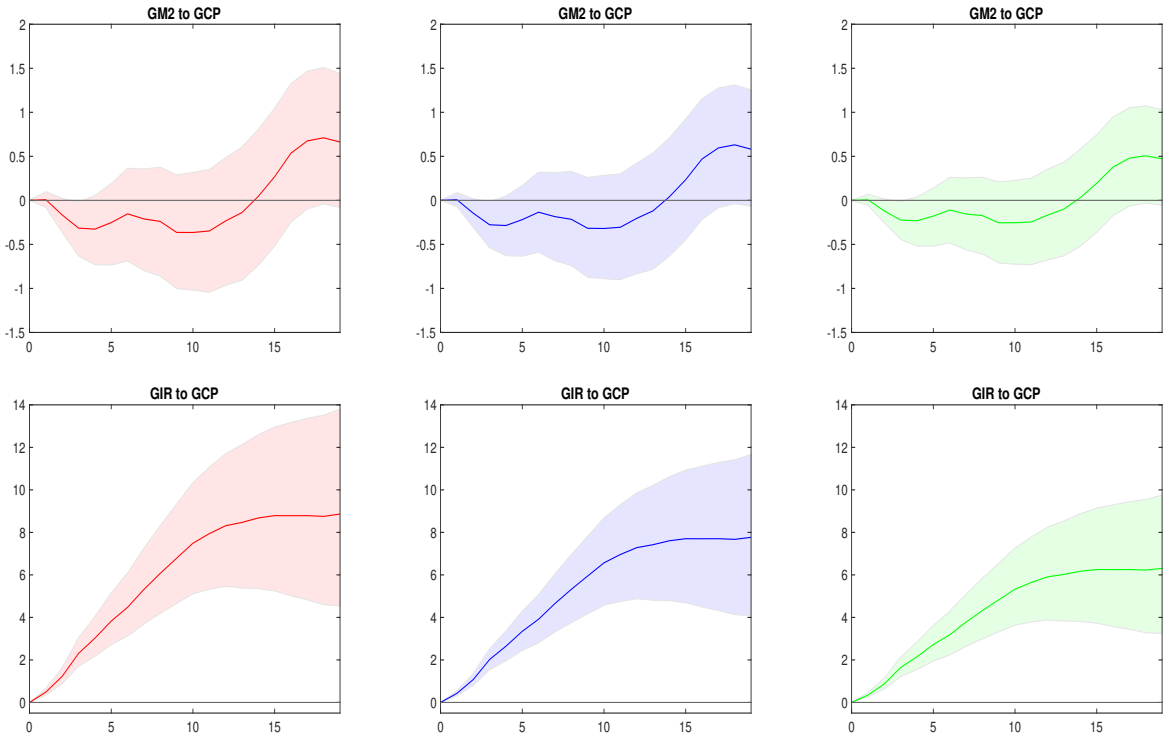

Figure 8: The first and second rows represent the impulse response functions (IRFs) of the global money supply (GM2) and the global interest rate (GIR) to a commodity price (GCP) shock, respectively. Each column reports the IRFs in a specific regime. Particularly, on the left are the IRFs in the first regime, on the right are the IRFs in the third regime, and in the middle are the IRFs in the second regime. The solid lines are the median responses, whereas the shaded areas correspond to 68% credible intervals.

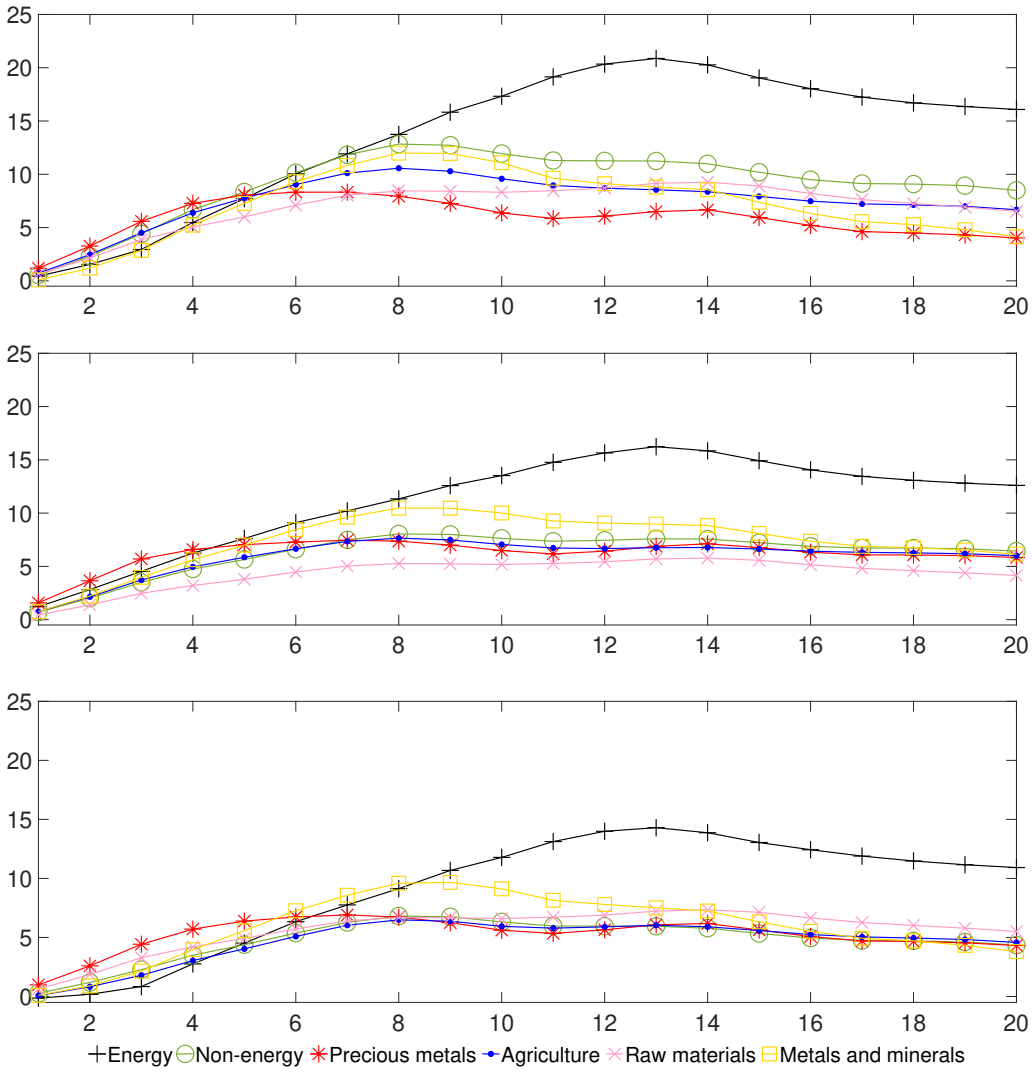

Figure 9: Upper panel: Cumulated impulse response functions of energy, non-energy, precious metals, agriculture, raw materials, and metals and minerals to a global money supply shock in the first regime. Middle panel: Cumulated impulse response functions of energy, non-energy, precious metals, agriculture, raw materials, and metals and minerals to a global money supply shock in the second regime. Lower panel: Cumulated impulse response functions of energy, non-energy, precious metals, agriculture, raw materials, and metals and minerals to a global money supply shock in the third regime.

APPENDIX

A Priors

This Appendix shows the priors that we use to estimate the MS-VAR model.

Prior specification for regime-independent parameters: The prior distribution of regime-independent autoregressive coefficients, $\boldsymbol{\gamma}_0$, is:

$$\boldsymbol{\gamma}_0 \sim \mathcal{N}_{K^2P}(\underline{\boldsymbol{\gamma}}_0, \underline{\boldsymbol{\Sigma}}_0), \tag{13}$$

where $\underline{\boldsymbol{\gamma}}_0 = \mathbf{0}_{K^2P}$, a $K^2P \times 1$ null vector, and $\underline{\boldsymbol{\Sigma}}_0 = 10\mathbf{I}_{K^2P}$.

Prior specification for the regime-dependent intercepts: The prior distribution of the MS intercepts, $\boldsymbol{\gamma}_i$, is:

$$\boldsymbol{\gamma}_i \sim \mathcal{N}_K(\underline{\boldsymbol{\gamma}}_i, \underline{\boldsymbol{\Sigma}}_i), \quad \text{for} \quad i = 1, \ldots, M, \tag{14}$$

where $\underline{\boldsymbol{\gamma}}_i = \mathbf{0}_K$, a $K \times 1$ null vector, and $\underline{\boldsymbol{\Sigma}}_i = 10\mathbf{I}_K$.

Prior specification for the regime dependent variance-covariance matrices: The prior chosen for the inverse of the regime-specific variance-covariance matrices is independent Wishart ($\mathcal{W}$) priors, which read as:

$$\boldsymbol{\Sigma}_i^{-1} \sim \mathcal{W}_K(\underline{\boldsymbol{\Upsilon}}_i, \underline{\nu}_i) \quad \text{for} \quad i = 1, \ldots, M \tag{15}$$

where $\underline{\nu}_i = 5$ is the degrees of freedom parameter and $\underline{\Upsilon}_i = 10\mathbf{I}_K$ is the scale matrix.

Prior specification for the parameters of the time-varying transition probabilities matrix: To avoid overfitting, following Billio et al. (2016), we use a hierarchical prior specification for the parameters of the Logit specification in time-varying transition probabilities. Specifically, for the parameters which drive the j-th row in the matrix in

Equation (2), we assume:

$$\begin{aligned} \boldsymbol{\theta}^{ij} &\sim \mathcal{N}_{N+1}\left(\boldsymbol{\psi}, \boldsymbol{\Omega}\right) \quad i = 1, \ldots, M-1 \\ \boldsymbol{\psi} &\sim \mathcal{N}_{N+1}(\underline{\boldsymbol{\psi}}, \underline{\boldsymbol{\Omega}}) \end{aligned} \tag{16}$$

with $\underline{\boldsymbol{\psi}} = \mathbf{0}_N$, a $N \times 1$ null vector, $\boldsymbol{\Omega} = \mathbf{I}_{N+1}$ and $\underline{\boldsymbol{\Omega}} = 10\mathbf{I}_{N+1}$.

B Posteriors

Posterior of the regime-independent parameters: The posterior distribution of the regime-independent parameter, $\boldsymbol{\gamma}_0$, is Normal with density function:

$$\begin{aligned} &f\left(\boldsymbol{\gamma}_0 \mid \mathbf{y}, \boldsymbol{\Xi}, \boldsymbol{\gamma}, \boldsymbol{\Sigma}, \underline{\boldsymbol{\gamma}_0}\right) \propto \\ &\propto \exp\left\{-\frac{1}{2}\boldsymbol{\gamma}_0'\left(\sum_{t=1}^{T}\mathbf{X}_{0t}'\boldsymbol{\Sigma}_t^{-1}\mathbf{X}_{0t} + \underline{\boldsymbol{\Sigma}}_0^{-1}\right)\boldsymbol{\gamma}_0 + \boldsymbol{\gamma}_0\left(\sum_{t=1}^{T}X_{0t}'\boldsymbol{\Sigma}_t^{-1}\mathbf{y}_{0t} + \underline{\boldsymbol{\Sigma}}_0^{-1}\underline{\boldsymbol{\gamma}}_0\right)\right\} \\ &\propto \mathcal{N}_{K^2P}\left(\bar{\boldsymbol{\gamma}}_0, \bar{\boldsymbol{\Sigma}}_0\right), \end{aligned} \tag{17}$$

where $\mathbf{y}_{0t} = \mathbf{y}_t - \sum_{i=1}^{M}\xi_{it}\mathbf{X}_{it}\boldsymbol{\gamma}_i$, $\bar{\boldsymbol{\gamma}}_0 = \bar{\boldsymbol{\Sigma}}_0\left(\underline{\boldsymbol{\Sigma}}_0^{-1}\underline{\boldsymbol{\gamma}}_0 + \sum_{t=1}^{T}\mathbf{X}_{0t}'\boldsymbol{\Sigma}_t^{-1}\mathbf{X}_{0t}\right)$, and $\bar{\boldsymbol{\Sigma}}_0^{-1} = (\underline{\boldsymbol{\Sigma}}_0^{-1} + \sum_{t=1}^{T}\mathbf{X}_{0t}'\boldsymbol{\Sigma}_t^{-1}\mathbf{X}_{0t})$

Posterior of the regime dependent intercepts: The conditional posterior distributions of $\boldsymbol{\gamma}_i$, with $i = 1, \ldots, M$, are normal with density functions:

$$\begin{aligned} &f\left(\boldsymbol{\gamma}_i \mid \mathbf{y}, \boldsymbol{\Xi}, \boldsymbol{\gamma}_0, \boldsymbol{\gamma}_{(-i)}, \boldsymbol{\Sigma}, \underline{\boldsymbol{\gamma}_i}\right) \propto \\ &\propto \exp\left\{-\frac{1}{2}\boldsymbol{\gamma}_i'\left(\sum_{t\in\mathcal{T}_i}\mathbf{X}_{it}'\boldsymbol{\Sigma}_t^{-1}\mathbf{X}_{it} + \underline{\boldsymbol{\Sigma}}_i^{-1}\right)\boldsymbol{\gamma}_i + \boldsymbol{\gamma}_i'\left(\sum_{t\in\mathcal{T}_i}\mathbf{X}_{it}'\boldsymbol{\Sigma}_t^{-1}\mathbf{y}_{it} + \underline{\boldsymbol{\Sigma}}_i^{-1}\underline{\boldsymbol{\gamma}}_i\right)\right\} \\ &\propto \mathcal{N}_K\left(\bar{\boldsymbol{\gamma}}_i, \bar{\boldsymbol{\Sigma}}_i\right) \end{aligned} \tag{18}$$

with $\overline{\boldsymbol{\gamma}}_i = \bar{\boldsymbol{\Sigma}}_i^{-1}\left(\underline{\boldsymbol{\Sigma}}_i^{-1}\underline{\boldsymbol{\gamma}}_i + \sum_{t\in\mathcal{T}_i}\mathbf{X}_{it}'\boldsymbol{\Sigma}_t^{-1}\mathbf{X}_{it}\right)$ and $\bar{\boldsymbol{\Sigma}}_i^{-1} = \left(\underline{\boldsymbol{\Sigma}}_i^{-1} + \sum_{t\in\mathcal{T}_i}\mathbf{X}_{it}'\boldsymbol{\Sigma}_t^{-1}\mathbf{X}_{it}\right)$ where $\mathcal{T}_i = \{t \mid \xi_{it} = 1, t = 1, \ldots, T\}$ and $\mathbf{y}_{it} = \mathbf{y}_t - \mathbf{X}_{0t}\boldsymbol{\gamma}_0$.

Posterior of the regime dependent variance-covariance matrices: The conditional posterior distribution of the regime-dependent variance-covariance matrix, $\boldsymbol{\Sigma}_i$, with $i = 1, \ldots, M$, are $\mathcal{W}$ densities:

$$\begin{aligned} & f(\boldsymbol{\Sigma}_i^{-1} \mid \mathbf{y}, \boldsymbol{\Xi}, \boldsymbol{\gamma}_0, \boldsymbol{\gamma}_i, \boldsymbol{\Sigma}_{(-i)}, \underline{\boldsymbol{\Upsilon}}_i) \propto \\ & \propto \mid \boldsymbol{\Sigma}_i^{-1} \mid^{\frac{\nu_i + T_i - K - 1}{2}} \exp\left\{ -\frac{1}{2} \mathrm{tr}\left(\left(\underline{\boldsymbol{\Upsilon}}_i^{-1} + \sum_{t \in \mathcal{T}_i} \mathbf{u}_{it} \mathbf{u}_{it}' \right) \boldsymbol{\Sigma}_i^{-1} \right) \right\} \\ & \propto \mathcal{W}_K(\bar{\nu}_i, \bar{\boldsymbol{\Upsilon}}_i) \end{aligned} \tag{19}$$

where $T_i = \sum_{t=1}^{T} \mathbb{I}_{\xi_{it}=1}$, $\mathbf{u}_{it} = \mathbf{y}_t - \mathbf{X}_{0t}\boldsymbol{\gamma}_0 - X_{it}\boldsymbol{\gamma}_i$, $\bar{\nu}_i = \underline{\nu}_i + T_i$, and $\bar{\boldsymbol{\Upsilon}}_i = \underline{\boldsymbol{\Upsilon}}_i + \sum_{t \in \mathcal{T}_i} \mathbf{u}_{it}\mathbf{u}_{it}'$.

Posterior of the parameters of the time-varying transition probabilities matrix: The full conditional distribution of the parameters in the j-th row of the transition matrix is:

$$f\left(\boldsymbol{\theta}^{j1}, \ldots, \boldsymbol{\theta}^{j(M-1)} | \mathbf{y}, \boldsymbol{\Xi}, \boldsymbol{\gamma}_i \right) \propto \prod_{t=1}^{T} \prod_{i=1}^{M-1} \left(G\left(\mathbf{V}_t, \boldsymbol{\theta}^{ki} \right) \right)^{\xi_{it}\xi_{jt-1}}, \tag{20}$$

and we apply Metropolis-Hastings.

C IRFs of commodity sectors

First regime												
Horizon	4			8			12			16		
	LB	Median	UB	LB	Median	UB	LB	Median	UB	LB	Median	UB
Energy	-0.8	5.5	11.9	2.6	13.7	25.1	4.5	20.3	36.4	-2.5	18.0	38.7
Non-Energy	3.4	6.7	10.1	6.9	12.8	19.1	2.5	11.3	20.3	-2.1	9.5	21.2
Precious metals	4.6	7.3	10.1	2.6	7.9	13.6	-2.1	6.1	14.5	-5.8	5.2	16.3
Agriculture	4.0	6.4	9.1	6.1	10.6	15.6	2.0	8.7	15.9	-1.5	7.5	16.8
Raw Materials	3.3	5.1	7.0	5.1	8.4	12.2	3.5	8.7	14.2	1.3	8.2	15.5
Metals and minerals	1.4	5.2	9.1	4.4	12.0	19.9	-2.3	9.1	21.0	-8.8	6.3	21.7
Second regime												
Horizon	4			8			12			16		
	LB	Median	UB	LB	Median	UB	LB	Median	UB	LB	Median	UB
Energy	3.2	6.2	9.4	5.3	11.3	17.5	6.7	15.6	24.7	2.3	14.1	26.0
Non-Energy	3.6	4.7	5.9	5.8	8.0	10.3	4.0	7.4	10.9	2.2	6.9	11.6
Precious metals	4.4	6.6	8.4	3.6	7.4	10.7	1.2	6.4	11.3	-0.4	6.3	12.8
Agriculture	3.8	4.9	6.1	5.4	7.7	10.0	3.2	6.7	10.2	1.8	6.4	11.1
Raw Materials	2.1	3.2	4.3	3.2	5.3	7.4	2.3	5.4	8.6	1.0	5.1	9.3
Metals and minerals	3.6	5.6	7.8	6.4	10.5	14.8	2.8	9.1	15.7	-5.7	7.4	16.0
Third regime												
Horizon	4			8			12			16		
	LB	Median	UB	LB	Median	UB	LB	Median	UB	LB	Median	UB
Energy	-0.7	2.8	6.7	2.0	9.1	17.2	3.5	14.0	25.8	-1.6	12.4	27.7
Non-Energy	2.3	3.5	4.7	4.4	6.8	9.6	2.2	6.0	9.9	-0.2	4.9	10.2
Precious metals	2.9	5.7	8.9	2.0	6.7	11.9	-1.3	5.6	12.9	-3.9	5.1	14.4
Agriculture	1.2	3.0	5.3	3.0	6.5	10.7	0.8	5.9	11.9	-1.5	5.2	13.0
Raw Materials	1.6	4.2	7.0	2.8	6.7	11.0	1.7	6.9	12.5	0.1	6.6	13.6
Metals and minerals	1.5	4.0	6.7	4.3	9.6	15.5	-0.7	7.8	16.6	-5.9	5.5	16.9

Table 4: Median impulse response functions. The table shows values of median impulse response functions, together with respective 68% confidence bandwidths in each regime; LB stands for the lower bound, while UB stands for the upper bound.